

# A one-dimensional computational model for the interaction of phase-transformations and plasticity

Richard Ostwald<sup>a,\*</sup>, Thorsten Bartel<sup>a</sup>, Andreas Menzel<sup>a,b</sup>

<sup>a</sup>*Institute of Mechanics, TU Dortmund, Leonhard-Euler-Str. 5, D-44227 Dortmund, Germany*

<sup>b</sup>*Division of Solid Mechanics, Lund University, P.O. Box 118, SE-22100 Lund, Sweden*

---

## Abstract

In this work, we model the basic mechanisms of the interaction between phase-transformations and plasticity within a one-dimensional constitutive framework. Efficient algorithms are presented, facilitating to solve the underlying evolution equations with high numerical stability at low numerical costs. Furthermore, a family of functions covering physically reasonable classes for the inheritance of plasticity in the context of evolving phases is proposed and discussed by means of several representative numerical examples.

*Key words:* Phase-transformations, Plasticity, Mixture-theory

---

## 1. Introduction

Functional materials like TRIP-steels and shape memory alloys offer a great potential for the industrial manufacturing of sophisticated components benefitting from the advantages that these materials can provide, such as locally varying hardness and stiffness. The need of a reliable manufacturing and application of such components leads to the demand of accurate constitutive models not only to predict the material's response by means of simulations, but also in view of material and structural design purposes. However, the coupling of phase-transformations and plasticity involves the interaction of multiple complex physical mechanisms, which have not yet been completely understood.

Micromechanically motivated material models are characterized by considering the microstructure of a material and its stress- or temperature-driven evolution. As shown in Bain (1924) and Bowles and MacKenzie (1954), in particular the kinematics of martensitic (i.e. diffusionless) solid-solid phase-transformations are characterized by homogeneous deformations of the crystal lattice. Thus, the transformation kinematics can be captured by so-called Bain-strains represented for example by the right stretch tensor  $\mathbf{U}^{\text{tr}}$  in a continuum mechanical context (see for example James and Hane (2000); Bhattacharya (2003)). Besides that, the material's microstructure can be approximately accounted for by matrix-inclusion homogenization schemes as suggested in Sun *et al.* (1991); Sun and Hwang (1993); Cherkaoui *et al.* (2000). These schemes approximate effective material properties for the phase mixture being bounded by the Voigt and Reuss limits, respectively. In this regard, a promising method for the determination of a suitable effective material response is referred to as energy relaxation.

The concept of energy relaxation is dedicated to the computation of the quasiconvex energy hull of an underlying multi-well free energy potential. It offers the possibility to predict the energetically most favorable arrangement of the underlying microstructure. A comprehensive treatise on quasiconvex analysis can be found

---

\*Corresponding author. Email: [richard.ostwald@udo.edu](mailto:richard.ostwald@udo.edu)

in Morrey (1952); Ball (1977); Dacorogna (1989) among others. Since the exact determination of the desired energy hull is only possible in rare cases as e.g. shown in Kohn (1991); DeSimone and Dolzmann (1999), the quasiconvexification is mostly approximated by upper and lower bounds as shown in Pagano *et al.* (1998); Ortiz and Repetto (1999); Stupkiewicz and Petryk (2002); Miehe *et al.* (2004). An extension of the energy relaxation concept has recently been presented in Bartel and Hackl (2009), where the deformations within each phase are directly derived from a superimposed displacement fluctuation field. Moreover, a distinction between elastic and dissipative internal variables is introduced therein in order to, on the one hand, determine a well-suited energy hull while, on the other hand, being able to account for the hysteretic behaviour of shape memory alloys. In this context, the evolution of dissipative variables can be established by ordinary differential equations derived from inelastic potentials according to e.g. Mielke and Theil (1999); Mielke *et al.* (2002).

The mentioned micromechanically motivated models are mainly based on the minimization of total energy and total power, respectively. In contrast to this, the models presented in Berezovski and Maugin (2007); Maugin and Berezovski (2009); Abeyaratne and Knowles (1990, 1993, 1997) are based on the derivation of driving forces directly acting on the propagating phase front. However, the increase of accuracy and physical plausibility enabled by micromechanical models is always accompanied by a significant increase of computational effort. In particular, the determination of energetically favorable arrangements of phases subjected to compatibility conditions (rank-one connections) leads to immense numerical costs. Moreover, micromechanical models are usually capable of simulating the behaviour of single crystals—in order to extend these models to polycrystalline materials, appropriate scale-bridging methods are required. Thus, the computation of large macroscopic problems—for example in the context of finite element simulations—is often realized using phenomenological approaches. These approaches, as for example introduced in Helm and Haupt (2003); Auricchio and Taylor (1997); Raniecki *et al.* (1992), are mainly based on thermodynamics. In addition to the first and second law of thermodynamics, the concept of generalized irreversible forces and fluxes, as established in Truesdell and Toupin (1960) amongst others, is used in order to derive evolution equations for the internal variables. An extension of the model proposed in Raniecki *et al.* (1992) has been presented in Müller and Bruhns (2006) in terms of finite strains and a self-consistent Eulerian theory accounting for heat generation during phase-transformations.

Another class of thermodynamical models is related to statistical considerations, resulting in transformation probabilities. As for example elaborated in Achenbach (1989); Abeyaratne and Knowles (1993); Huo and Müller (1993); Abeyaratne *et al.* (1994); Seelecke (1996); Müller and Seelecke (2001), these models are based on multi-well Helmholtz free energy potentials. The nucleation criteria are formulated in terms of energy barriers, which lead to statistically derived transformation probabilities governing—together with Boltzmann-based transition attempt frequencies, see e.g. Govindjee and Hall (2000)—the evolution of material phases.

The goal of this contribution is to enhance the statistics-based phase-transformation model described in Govindjee and Hall (2000); Ostwald *et al.* (2010) in order to take into account plasticity as well as the interaction between phase-transformation and plasticity effects by introducing a so-called plastic inheritance law. The model is presented in Section 2, where extended Helmholtz free energy functions for each material phase are presented, taking into account plastic strains as new variables for each individual phase. Based on the extended multi-well energy potentials, the probabilistic phase-transformation model is derived in Section 2.1. Moreover, the differential equations describing the evolution of plasticity as well as the potential-based derivation of the individual plastic driving forces are shown in Section 2.2 and 2.2.1, respectively. The coupling of phase-transformation and plasticity effects is incorporated by means of a staggered algorithm. To this end, an inheritance algorithm for the inheritance of plastic strains resulting from a propagating phase front is introduced in Section 2.3. Moreover, two physically reasonable exponential-type inheritance probability functions are presented in Section 2.3.1 and 2.3.2. Details on the numerical implementation of the model are provided in Section 3, followed by numerical examples shown in Section 4, where the model is applied not only to shape memory alloys (see Section 4.2), but also to TRIP steel (see Section 4.3). It is shown that the model nicely reflects the actual physical behaviour of both types of materials.

## 2. A model for the interaction of phase-transformations and plasticity

The one-dimensional phase-transformation model is based on mixture theory, where we make use of the Voigt assumption, i.e. all material phases are subject to the same strain  $\varepsilon$ . The implemented phase-transformation model is capable of handling an arbitrary amount of material phases, where the volume fraction

$$\xi^\alpha \stackrel{\text{def}}{=} \lim_{v \rightarrow 0} \left( \frac{v^\alpha}{v} \right) \quad (1)$$

of each phase  $\alpha \in \{1, \dots, \nu\} \subset \mathbb{N}$  is subject to the restrictions

$$\xi^\alpha \in [0, 1] \subset \mathbb{R} \quad , \quad \sum_{\alpha} \xi^\alpha = 1 \quad , \quad \sum_{\alpha} \dot{\xi}^\alpha = 0 \quad . \quad (2)$$

While the validity of (2)<sub>a</sub> and (2)<sub>b</sub> is evident, (2)<sub>c</sub> follows from mass conservation. Each phase is presumed to behave thermo-elasto-plastically, thus a Helmholtz free energy function  $\psi^\alpha = \widehat{\psi}^\alpha(\varepsilon, \varepsilon_{\text{pl}}^\alpha, \theta)$  of the form

$$\begin{aligned} \rho_0 \psi^\alpha &= \frac{1}{2} \mathbb{E}^\alpha [\varepsilon - \varepsilon_{\text{tr}}^\alpha - \varepsilon_{\text{pl}}^\alpha]^2 - \zeta^\alpha \mathbb{E}^\alpha [\varepsilon - \varepsilon_{\text{tr}}^\alpha - \varepsilon_{\text{pl}}^\alpha] [\theta - \theta_0] \\ &+ \rho_0 c_p^\alpha \theta \left[ 1 - \log \left( \frac{\theta}{\theta_0} \right) \right] - \rho_0 \lambda_T^\alpha \left[ 1 - \frac{\theta}{\theta_0} \right] \end{aligned} \quad (3)$$

is assigned to each phase  $\alpha$ , with  $\mathbb{E}$  the Young's modulus,  $\varepsilon = \nabla_x u$  the total strains,  $\varepsilon_{\text{tr}}$  the transformation strains,  $\varepsilon_{\text{pl}}$  the plastic strains,  $\zeta$  the coefficient of thermal expansion,  $\theta$  the current absolute temperature,  $\theta_0$  the reference temperature,  $c_p$  the heat capacity, and  $\lambda_T$  the latent heat of the respective material phase. The overall free energy of the mixture  $\Psi = \widehat{\Psi}(\varepsilon, \varepsilon_{\text{pl}}^{\text{1d}}, \theta, \boldsymbol{\xi}) = \sum_{\alpha} \xi^\alpha \psi^\alpha$ , with  $\boldsymbol{\xi} = [\xi^1, \dots, \xi^\nu]$  and  $\varepsilon_{\text{pl}}^{\text{1d}} = [\varepsilon_{\text{pl}}^1, \dots, \varepsilon_{\text{pl}}^\nu]$ , can directly be obtained from the free energy contributions of the respective constituents, since the distortional energy of the phase boundaries is neglected here.

Based on this, the Gibbs potential  $G = \widehat{G}(\partial\Psi/\partial\varepsilon, \boldsymbol{\xi}, \theta)$  can be obtained by carrying out a Legendre-transformation, i.e.

$$G = - \sup_{\varepsilon} \left( \left. \frac{\partial \widehat{\Psi}(\varepsilon, \varepsilon_{\text{pl}}^{\text{1d}}, \theta, \boldsymbol{\xi})}{\partial \varepsilon} \right|_{\theta, \varepsilon_{\text{pl}}^{\text{1d}}} \varepsilon - \rho_0 \Psi \right) \quad (4)$$

$$= - \sup_{\varepsilon} \left( \sum_{\alpha} \xi^\alpha [\sigma \varepsilon - \rho_0 \psi^\alpha] \right) \quad (5)$$

$$= - \sup_{\varepsilon} \left( \sum_{\alpha} \xi^\alpha g^\alpha \right) \quad , \quad (6)$$

where  $\sigma = \partial\Psi/\partial\varepsilon|_{\theta, \varepsilon_{\text{pl}}^{\text{1d}}} = \widehat{\sigma}(\varepsilon, \varepsilon_{\text{pl}}^{\text{1d}}, \boldsymbol{\xi}, \theta)$  is the stress acting in the one-dimensional continuum considered and  $g^\alpha = \widehat{g}^\alpha(\sigma, \varepsilon, \varepsilon_{\text{pl}}^\alpha, \theta) \stackrel{\text{def}}{=} \sigma \varepsilon - \rho_0 \psi^\alpha$  represents the contribution of phase  $\alpha$  to the overall Gibbs potential  $G$ .

### 2.1. Evolution of volume fractions

For the evolution of the volume fractions  $\xi^\alpha$  we use an approach based on statistical physics. In this regard, a transformation probability matrix  $\mathbf{Q}_\nu \in \mathbb{R}^{\nu \times \nu}$  introduced in Govindjee and Hall (2000) is used, facilitating to derive the evolution of volume fractions as

$$\dot{\boldsymbol{\xi}} = \mathbf{Q}_\nu \cdot \boldsymbol{\xi} \quad , \quad (7)$$

wherein the notation  $\dot{\bullet}$  denotes the material time derivative. Since we restrict ourselves to two material phases in this work, namely austenite (A) and martensite (M), the according transformation probability matrix  $\mathbf{Q}_2 \in \mathbb{R}^{2 \times 2}$  reduces to

$$\mathbf{Q}_2 = \omega \begin{bmatrix} -P_{A \rightarrow M} & P_{M \rightarrow A} \\ P_{A \rightarrow M} & -P_{M \rightarrow A} \end{bmatrix} \neq \mathbf{Q}_2^t \quad (8)$$

with  $\omega$  the transition attempt frequency and  $P_{\alpha \rightarrow \beta} = \widehat{P}_{\alpha \rightarrow \beta}(\theta, b_{\alpha \rightarrow \beta})$  the probability of a transformation of one phase  $\alpha$  to the other phase  $\beta$ . Note that (8) refers to  $\boldsymbol{\xi} = [\xi^A, \xi^M]^t \in \mathbb{R}^2$ . Furthermore,  $\sum_i Q_{ij} = 0 \forall j$  guarantees that (2)<sub>c</sub> is fulfilled.

According to Achenbach (1989), the transformation probabilities necessary to assemble  $\mathbf{Q}_\bullet$  can be obtained from

$$P_{\alpha \rightarrow \beta} = \exp\left(\frac{-\Delta v b_{\alpha \rightarrow \beta}}{k \theta}\right), \quad (9)$$

with  $\Delta v$  the constant transformation region's volume,  $b_{\alpha \rightarrow \beta}$  the energy barrier for the transformation from phase  $\alpha$  to phase  $\beta$ ,  $k$  the Boltzmann's constant, and  $\theta$  the given temperature. Note that, in general,  $b_{\alpha \rightarrow \beta} \neq b_{\beta \rightarrow \alpha}$  and thus  $P_{\alpha \rightarrow \beta} \neq P_{\beta \rightarrow \alpha}$  holds. The energy barriers can be determined from

$$b_{\alpha \rightarrow \beta} = \widehat{g}^\alpha(\sigma, \varepsilon_{\alpha, \beta}^*, \theta) - \widehat{g}^\alpha(\sigma, \varepsilon_\alpha^{\min}, \theta) \quad (10)$$

with

$$\varepsilon_{\alpha, \beta}^* = \inf_{g^\alpha, g^\beta} \left\{ \varepsilon \mid \widehat{g}^\alpha(\sigma, \varepsilon, \theta)|_{\sigma, \theta} = \widehat{g}^\beta(\sigma, \varepsilon, \theta)|_{\sigma, \theta} \right\} \quad (11)$$

and

$$\varepsilon_\alpha^{\min} = \left\{ \varepsilon \mid \left. \frac{\partial \widehat{g}^\alpha(\sigma, \varepsilon, \theta)}{\partial \varepsilon} \right|_{\sigma, \theta} = 0 \right\}, \quad (12)$$

where  $\widehat{g}^\alpha(\sigma, \varepsilon_{\alpha, \beta}^*, \theta) = \widehat{g}^\beta(\sigma, \varepsilon_{\alpha, \beta}^*, \theta)$  gives the value of the energy potentials at the intersection of the parabolic phase potential functions for two material phases ( $\alpha, \beta$ ) in strain space, while  $\widehat{g}^\alpha(\sigma, \varepsilon_\alpha^{\min}, \theta)$  denotes the minimum energy potential of a particular phase  $\alpha$  for fixed stresses and temperature. Accordingly, the difference of both energy values (10) gives the energy barrier that has to be overcome for a transformation from phase  $\alpha$  to  $\beta$ .

## 2.2. Evolution of plastic strains

To incorporate plasticity, we—for conceptual simplicity—assume von Mises-type plasticity with linear proportional hardening. Based on the overall free energy potential, the plastic driving force  $q_{\text{pl}, \psi}^\alpha$  can be derived for each phase  $\alpha$ , see Section 2.2.1 for details. With the driving force and the current yield stress  $Y^\alpha$  at hand, the yield function  $\widehat{\Phi}^\alpha = \widehat{\Phi}^\alpha(Y^\alpha, q_{\text{pl}, \psi}^\alpha)$  determining the admissible elastic domain in phase  $\alpha$ , is given as

$$\widehat{\Phi}^\alpha(q_{\text{pl}, \psi}^\alpha, Y^\alpha) = |q_{\text{pl}, \psi}^\alpha - \xi^\alpha b^\alpha| - \xi^\alpha Y^\alpha \leq 0 \quad (13)$$

The current yield stress  $Y^\alpha = \widehat{Y}^\alpha(\gamma^\alpha) = Y_0^\alpha + H^\alpha \gamma^\alpha$  is given by the initial yield stress  $Y_0^\alpha$  being modified by  $H^\alpha \gamma^\alpha$  due to accumulated plastic strains  $\gamma^\alpha$  of the respective material phase, where  $H^\alpha$  denotes the constant hardening modulus of phase  $\alpha$ . The individual back stress  $\xi^\alpha b^\alpha$  is additionally considered in order to prevent plastic flow occurring in the initial equilibrium state. To be specific, the underlying Voigt assumption leads to an initial stress of

$$\begin{aligned} b^\alpha &\stackrel{\text{def}}{=} \widehat{\sigma}^\alpha(\varepsilon = 0, \varepsilon_{\text{pl}}^\alpha = 0, \theta) \\ &= \left. \frac{\partial \widehat{\psi}^\alpha(\varepsilon, \varepsilon_{\text{pl}}^\alpha, \theta)}{\partial \varepsilon} \right|_{\theta, \varepsilon_{\text{pl}}^\alpha = 0, \varepsilon = 0} \\ &= -\mathbf{E}^\alpha \varepsilon_{\text{tr}}^\alpha + \zeta^\alpha \mathbf{E}^\alpha \varepsilon_{\text{tr}}^\alpha [\theta - \theta_0] \end{aligned} \quad (14)$$

that acts in each phase  $\alpha$  and, in consequence, is considered as a back stress in the yield function. Based on the yield function presented, we make use of an associated flow rule, facilitating to derive the evolution law for the plastic strain in phase  $\alpha$  by means of

$$\dot{\varepsilon}_{\text{pl}}^\alpha = \dot{\lambda}^\alpha \frac{\partial \widehat{\Phi}^\alpha(q_{\text{pl}, \psi}^\alpha, Y^\alpha)}{\partial q_{\text{pl}, \psi}^\alpha} = \dot{\lambda}^\alpha \text{sgn}(q_{\text{pl}, \psi}^\alpha - \xi^\alpha b^\alpha) \quad (15)$$

with an appropriate Lagrangian multiplier  $\dot{\lambda}^\alpha$ .

### 2.2.1. Remarks on the derivation of the plastic driving force

The stress-type force  $q_{\text{pl},\Psi}^\alpha = \widehat{q}_{\text{pl},\Psi}^\alpha(\xi^\alpha, \varepsilon, \varepsilon_{\text{pl}}^\alpha, \theta)$  driving the evolution of plasticity in phase  $\alpha$  can be derived from the overall free energy  $\Psi$  according to

$$q_{\text{pl},\Psi}^\alpha = - \left. \frac{\partial \widehat{\Psi}(\varepsilon, \varepsilon_{\text{pl}}^{\text{1d}}, \theta, \boldsymbol{\xi})}{\partial \varepsilon_{\text{pl}}^\alpha} \right|_{\theta, \varepsilon, \boldsymbol{\xi}} \quad (16)$$

$$= - \left. \frac{\partial}{\partial \varepsilon_{\text{pl}}^\alpha} \right|_{\theta, \varepsilon} \sum_{\alpha} \xi^\alpha \widehat{\psi}^\alpha(\varepsilon, \varepsilon_{\text{pl}}^\alpha, \theta) \quad (17)$$

$$= - \xi^\alpha \left. \frac{\partial \widehat{\psi}^\alpha(\varepsilon, \varepsilon_{\text{pl}}^\alpha, \theta)}{\partial \varepsilon_{\text{pl}}^\alpha} \right|_{\theta, \varepsilon}, \quad (18)$$

finally resulting in

$$q_{\text{pl},\Psi}^\alpha = \xi^\alpha [\mathbf{E}^\alpha[\varepsilon - \varepsilon_{\text{tr}}^\alpha - \varepsilon_{\text{pl}}^\alpha] + \zeta^\alpha \mathbf{E}^\alpha[\theta - \theta_0]] \quad (19)$$

Furthermore, the stress acting in the one-dimensional continuum is obtained from

$$\sigma = \left. \frac{\partial \widehat{\Psi}(\varepsilon, \varepsilon_{\text{pl}}^{\text{1d}}, \theta, \boldsymbol{\xi})}{\partial \varepsilon} \right|_{\theta, \varepsilon_{\text{pl}}^{\text{1d}}} \quad (20)$$

$$= \left. \frac{\partial}{\partial \varepsilon} \right|_{\theta, \varepsilon_{\text{pl}}^{\text{1d}}} \left[ \sum_{\alpha} \xi^\alpha \widehat{\psi}^\alpha(\varepsilon, \varepsilon_{\text{pl}}^\alpha, \theta) \right] \quad (21)$$

$$= \sum_{\alpha} \xi^\alpha \left. \frac{\partial \widehat{\psi}^\alpha(\varepsilon, \varepsilon_{\text{pl}}^\alpha, \theta)}{\partial \varepsilon} \right|_{\theta, \varepsilon_{\text{pl}}^\alpha} \quad (22)$$

$$= \sum_{\alpha} \xi^\alpha \sigma^\alpha \quad (23)$$

with  $\sigma^\alpha = \widehat{\sigma}^\alpha(\varepsilon, \varepsilon_{\text{pl}}^\alpha, \theta) = \mathbf{E}^\alpha[\varepsilon - \varepsilon_{\text{tr}}^\alpha - \varepsilon_{\text{pl}}^\alpha] + \zeta^\alpha \mathbf{E}^\alpha[\theta - \theta_0]$  the stress acting in phase  $\alpha$ . Comparing this result to (19) shows that  $q_{\text{pl},\Psi}^\alpha = \xi^\alpha \sigma^\alpha$ .

Alternatively, the plastic driving forces can be derived by considering each phase individually. Using this approach, the driving force  $q_{\text{pl},\psi}^\alpha = \widehat{q}_{\text{pl},\psi}^\alpha(\varepsilon, \varepsilon_{\text{pl}}^\alpha, \theta)$  yields

$$q_{\text{pl},\psi}^\alpha = - \left. \frac{\partial \widehat{\psi}^\alpha(\varepsilon, \varepsilon_{\text{pl}}^\alpha, \theta)}{\partial \varepsilon_{\text{pl}}^\alpha} \right|_{\theta, \varepsilon} \quad (24)$$

$$= \mathbf{E}^\alpha[\varepsilon - \varepsilon_{\text{tr}}^\alpha - \varepsilon_{\text{pl}}^\alpha] + \zeta^\alpha \mathbf{E}^\alpha[\theta - \theta_0] \quad (25)$$

$$= \sigma^\alpha \quad (26)$$

In particular, this result leads to  $q_{\text{pl},\Psi}^\alpha = \xi^\alpha q_{\text{pl},\psi}^\alpha$ . Note that the consideration of the volume fraction  $\xi^\alpha$  within the plastic driving force of each phase  $\alpha$  guarantees that  $\widehat{q}_{\text{pl},\Psi}^\alpha(\xi^\alpha = 0, \varepsilon, \varepsilon_{\text{pl}}^\alpha, \theta) = 0$ , and thus  $\dot{\varepsilon}_{\text{pl}}^\alpha = 0$  as long as  $\xi^\alpha = 0$ , i.e. no evolution of plasticity can occur within a phase of zero volume fraction.

### 2.3. Plastic inheritance

When the phase front of a phase  $\alpha$  evolves throughout a crystal from time step  ${}^n t$  to  ${}^{n+1} t$ , the question arises, whether plastic strains present in the decreasing phase  $\beta$  are inherited by the phase front of the increasing phase or not (see Figure 1). Conceptually speaking, one has to specify to which amount a positive volume fraction increment  $\Delta \xi^\alpha = {}^{n+1} \xi^\alpha - {}^n \xi^\alpha > 0$  of phase  $\alpha$  transfers plastic strains from phase  $\beta$  to phase  $\alpha$ . In general, the

updated plastic strains  $\tilde{\varepsilon}_{\text{pl}}^{\alpha} = \widehat{\tilde{\varepsilon}}_{\text{pl}}^{\alpha}(n\xi^{\alpha}, \Delta\xi^{\alpha}, \varepsilon_{\text{pl}}^{\alpha}, \varepsilon_{\text{pl}}^{\beta}, \Pi^{\beta \rightarrow \alpha})$  in phase  $\alpha$  can be determined via

$$\tilde{\varepsilon}_{\text{pl}}^{\alpha} = \frac{1}{n+1\xi^{\alpha}} \left[ n\xi^{\alpha} \varepsilon_{\text{pl}}^{\alpha} + \Pi^{\beta \rightarrow \alpha} \Delta\xi^{\alpha} \varepsilon_{\text{pl}}^{\beta} \right] \quad , \quad (27)$$

where  $\Pi^{\beta \rightarrow \alpha}$  reflects the probability of phase  $\alpha$  inheriting the dislocations present in phase  $\beta$  (see Figure 1). If one further assumes, that the diffusionless lattice shearing taking place during the phase-transformations considered neither generates nor annihilates any dislocations, i.e. the overall amount of plastic deformations remains constant in terms of

$$n+1\xi^{\alpha} \tilde{\varepsilon}_{\text{pl}}^{\alpha} + n+1\xi^{\beta} \tilde{\varepsilon}_{\text{pl}}^{\beta} = n\xi^{\alpha} \varepsilon_{\text{pl}}^{\alpha} + n\xi^{\beta} \varepsilon_{\text{pl}}^{\beta} \quad , \quad (28)$$

then the updated plastic deformations  $\tilde{\varepsilon}_{\text{pl}}^{\beta} = \widehat{\tilde{\varepsilon}}_{\text{pl}}^{\beta}(n\xi^{\beta}, \Delta\xi^{\alpha}, \varepsilon_{\text{pl}}^{\beta}, \Pi^{\beta \rightarrow \alpha})$  remaining in the decreased phase  $\beta$  are obtained from

$$\tilde{\varepsilon}_{\text{pl}}^{\beta} = \frac{1}{n+1\xi^{\beta}} \left[ n\xi^{\beta} - \Pi^{\beta \rightarrow \alpha} \Delta\xi^{\alpha} \right] \varepsilon_{\text{pl}}^{\beta} \quad . \quad (29)$$

As we restrict ourselves, for the sake of simplicity, to two phases, it is obvious that the increase  $\Delta\xi^{\alpha}$  of phase  $\alpha$  is related to the decrease  $\Delta\xi^{\beta}$  of phase  $\beta$  via

$$\Delta\xi^{\beta} = n+1\xi^{\beta} - n\xi^{\beta} = -\Delta\xi^{\alpha} \quad , \quad \Delta\xi^{\beta} < 0 \quad (30)$$

due to mass conservation, thus leading to

$$n+1\xi^{\beta} = n\xi^{\beta} - \Delta\xi^{\alpha} \quad . \quad (31)$$

Comparing (29) and (31) then shows that, in case of  $\Pi^{\beta \rightarrow \alpha} = 1$ , the plastic deformations in the decreasing phase are not affected by the change of volume fractions, i.e.  $\widehat{\tilde{\varepsilon}}_{\text{pl}}^{\beta}(n\xi^{\beta}, \Delta\xi^{\alpha}, \varepsilon_{\text{pl}}^{\beta}, \Pi^{\beta \rightarrow \alpha} = 1) = \varepsilon_{\text{pl}}^{\beta}$ . On the other hand, in case of  $\Pi^{\beta \rightarrow \alpha} = 0$ , i.e. if all dislocations are pushed rather than inherited by the propagating phase front of phase  $\alpha$ , the plastic strains in phase  $\beta$  increase inversely proportional to the decrease of volume fraction.

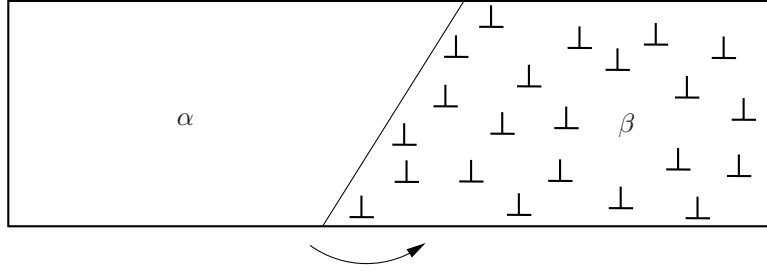
However, it is physically reasonable to assume that the inheritance probability is not constant, but rather a function depending on the remaining volume fraction  $\xi^{\beta}$  and plastic strain  $\varepsilon_{\text{pl}}^{\beta}$  of the decreasing phase  $\beta$ , as well as on further material parameters characterizing the actual functional dependency. To this end, two reasonable approaches for introducing exponential-type inheritance probability functions, namely a convex and a concave one,  $\Pi_{\text{cvx}}^{\beta \rightarrow \alpha} = \widehat{\Pi}_{\text{cvx}}^{\beta \rightarrow \alpha}(\xi^{\beta}, \varepsilon_{\text{pl}}^{\beta}; \kappa)$  and  $\Pi_{\text{ccv}}^{\beta \rightarrow \alpha} = \widehat{\Pi}_{\text{ccv}}^{\beta \rightarrow \alpha}(\xi^{\beta}, \varepsilon_{\text{pl}}^{\beta}; \kappa, \varepsilon_{\text{pl,sat}}^{\beta})$ , respectively, are presented in the following.

### 2.3.1. Convex inheritance probability function

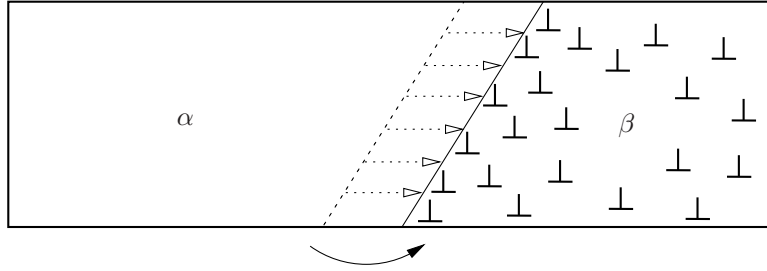
The inheritance probability function considered is subjected to two physically reasonable restrictions. First, in case that the volume fraction of the decreasing phase  $\beta$  is very large, i.e.  $\xi^{\beta} \approx 1$ , a propagating phase front of phase  $\alpha$  will most likely push dislocations present in phase  $\beta$ , since the dislocation density<sup>1</sup>—being inversely proportional to the volume fraction—in  $\beta$  is rather low in this case. In consequence and as the first condition, we require the inheritance probability function to match  $\widehat{\Pi}_{\text{cvx}}^{\beta \rightarrow \alpha}(\xi^{\beta} = 1, \varepsilon_{\text{pl}}^{\beta}; \kappa) = 0$ . On the other hand, if the remaining volume fraction  $\xi^{\beta}$  of the decreasing phase  $\beta$  tends to zero, the dislocation density takes high values so that the dislocations (or rather plastic strains) remaining in phase  $\beta$  are forced to be inherited by the evolving phase  $\alpha$ , i.e.  $\widehat{\Pi}_{\text{cvx}}^{\beta \rightarrow \alpha}(\xi^{\beta} = 0, \varepsilon_{\text{pl}}^{\beta}; \kappa) = 1$ . One exponential-type ansatz for an inheritance probability function fulfilling these restrictions is

$$\widehat{\Pi}_{\text{cvx}}^{\beta \rightarrow \alpha}(\xi^{\beta}, \varepsilon_{\text{pl}}^{\beta}; \kappa) = [1 - \xi^{\beta}] \exp\left(\frac{-\kappa \xi^{\beta}}{|\varepsilon_{\text{pl}}^{\beta}|}\right) \quad . \quad (32)$$

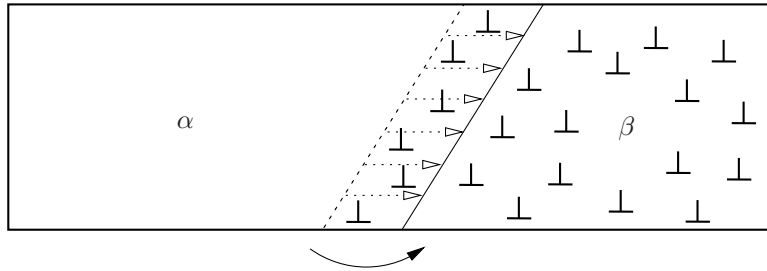
<sup>1</sup>The phrase *dislocation density* does not refer to  $\text{curl}(\boldsymbol{\varepsilon}_{\text{pl}})$ , respectively  $\partial_x \varepsilon_{\text{pl}}$  here. In the current context, we rather use this denomination as a synonym for the density of plastic strains.



(a) Initial state: the phase front of  $\alpha$  is about to move.



(b)  $\Pi^{\beta \rightarrow \alpha} = 0$ , i.e. all dislocations are pushed by the phase-front and remain within phase  $\beta$ .



(c)  $\Pi^{\beta \rightarrow \alpha} = 1$ , i.e. all dislocations within the volume that undergoes a phase-change are inherited to the growing phase  $\alpha$ .

Figure 1: Dislocations can either be inherited or pushed by the propagating phase front of an evolving phase  $\alpha$ . Here, the two special cases, i.e. no inheritance (b) and full inheritance (c) of dislocations during phase front propagation are shown. However, the actual physical behaviour of a material regarding inheritance of dislocations—or rather plastic strains—can be expected to lie in between both extreme cases. Therefore an inheritance probability function  $\Pi^{\beta \rightarrow \alpha} = \widehat{\Pi}^{\beta \rightarrow \alpha}(\xi^\beta, \varepsilon_{\text{pl}}^\beta; \dots) \in [0, 1] \subset \mathbb{R}$ , depending on the volume fraction  $\xi^\beta$  and plastic strain  $\varepsilon_{\text{pl}}^\beta$  of phase  $\beta$  as well as on material parameters, is introduced in this work (see Sections 2.3.1 and 2.3.2).

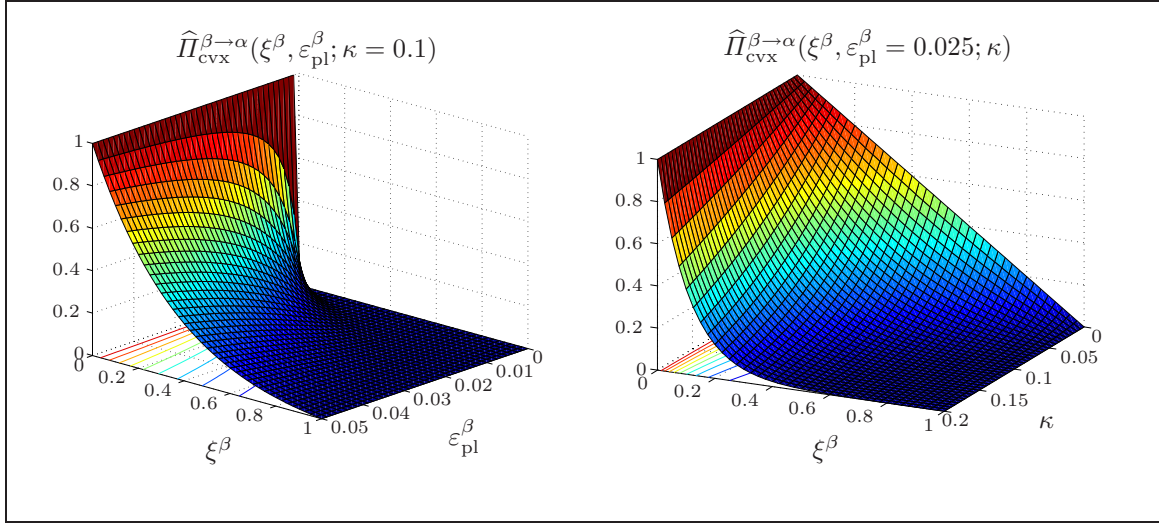


Figure 2: Convex inheritance probability function depending on volume fraction  $\xi^\beta$  and plastic strain  $\varepsilon_{\text{pl}}^\beta$  for given parameter  $\kappa = 0.1$  (left), and the function depending on  $\xi^\beta$  and  $\kappa$  for given plastic strain  $\varepsilon_{\text{pl}}^\beta = 0.025$  (right).

For an exemplary material parameter  $\kappa = 0.1$ , the development of this inheritance function is visualized in Figure 2. Besides that, the influence of the parameter  $\kappa$  for an exemplary fixed plastic strain of  $\varepsilon_{\text{pl}}^\beta = 0.025$  is displayed. As the figure shows, the proposed family of parametric inheritance functions is convex in  $\xi$  for all parameters  $\kappa \in \mathbb{R}^+$ .

### 2.3.2. Concave inheritance probability function

As an addition to the convex<sup>2</sup> inheritance probability function shown in Section 2.3.1, a concave<sup>2</sup> exponential-type inheritance function is presented in the following. As before, the physical restrictions, i.e.  $\hat{\Pi}_{\text{ccv}}^{\beta \rightarrow \alpha}(\xi^\beta = 1, \varepsilon_{\text{pl}}^\beta; \kappa) = 0$  and  $\hat{\Pi}_{\text{ccv}}^{\beta \rightarrow \alpha}(\xi^\beta = 0, \varepsilon_{\text{pl}}^\beta; \kappa) = 1$ , are required to be fulfilled. To be specific, the function

$$\hat{\Pi}_{\text{ccv}}^{\beta \rightarrow \alpha}(\xi^\beta, \varepsilon_{\text{pl}}^\beta; \kappa, \varepsilon_{\text{pl, sat}}^\beta) = \frac{1 - \exp\left(\frac{-\kappa [1 - \xi^\beta]}{\varepsilon_{\text{pl, sat}}^\beta - |\varepsilon_{\text{pl}}^\beta|}\right)}{1 - \exp\left(\frac{-\kappa}{\varepsilon_{\text{pl, sat}}^\beta - |\varepsilon_{\text{pl}}^\beta|}\right)}, \quad (33)$$

which again depends on a material parameter  $\kappa \in \mathbb{R}^+$ , is of exponential type, but provides a concave behaviour in  $\xi$ . As above, we require the inheritance probability to increase with increasing plastic strain. Accordingly, a plastic saturation strain  $\varepsilon_{\text{pl, sat}}^\beta \in \mathbb{R}^+$ , which can also be regarded as a material-dependent quantity, is introduced here. If the magnitude  $|\varepsilon_{\text{pl}}^\beta|$  of the plastic strain present in phase  $\beta$  reaches the saturation strain  $\varepsilon_{\text{pl, sat}}^\beta$ , the inheritance probability tends towards 1, i.e.  $\hat{\Pi}_{\text{ccv}}^{\beta \rightarrow \alpha}(\xi^\beta, \varepsilon_{\text{pl}}^\beta \rightarrow \varepsilon_{\text{pl, sat}}^\beta; \kappa, \varepsilon_{\text{pl, sat}}^\beta) \rightarrow 1 \forall \xi^\beta < 1$ . Figure 3 shows the development of the concave inheritance function for a given parameter of  $\kappa = 0.1$  and an exemplary saturation strain of  $\varepsilon_{\text{pl, sat}}^\beta = 0.05$ . Furthermore, the actual influence of  $\kappa$  on the inheritance probability function is presented for an exemplary plastic strain of  $\varepsilon_{\text{pl}}^\beta = 0.025$ .

<sup>2</sup>Here and in the following, by *convex* or *concave* inheritance functions, we mean convex or concave in  $\xi$ .

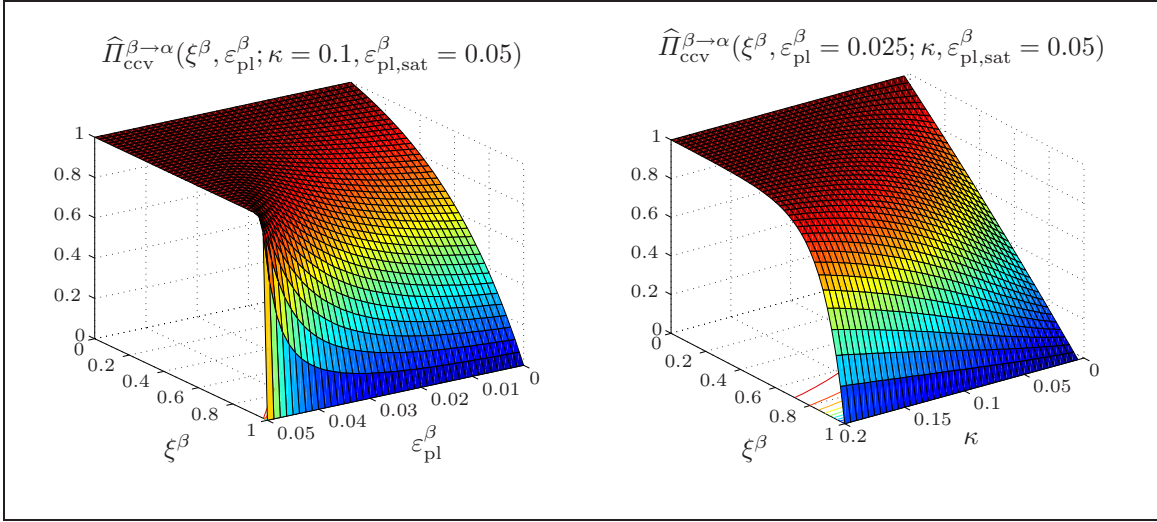


Figure 3: Concave inheritance probability function depending on volume fraction  $\xi^\beta$  and plastic strain  $\varepsilon_{\text{pl}}^\beta$  for given parameters  $\kappa = 0.1$  and  $\varepsilon_{\text{pl,sat}}^\beta = 0.05$  (left), and the function depending on  $\xi^\beta$  and  $\kappa$  for given plastic strain  $\varepsilon_{\text{pl}}^\beta = 0.025$  (right).

### 3. Numerical integration of evolution equations

The solution of the strongly non-linear system of evolution equations (7), required to obtain an update of the internal variables by means of volume fractions, is traditionally carried out using classical implicit integration schemes in combination with Newton-type iterations. In contrast to that, in the current work an explicit integration scheme, also discussed in Ostwald *et al.* (2010), is applied. The integration scheme is based on the assumption that the transformation rates of volume fractions  $\xi$  proceed linearly within a time step  $\Delta t = {}^{n+1}t - {}^n t > 0$ , i.e. from state  $n$  to  $n + 1$ . As shown in Ostwald *et al.* (2010), it is possible to obtain an explicit A-stable update using

$${}^{n+1}\xi = {}^n\xi + \frac{1}{2}\Delta t \left[ {}^{n+1}\dot{\xi} + {}^n\mathbf{Q} \cdot {}^n\xi \right] , \quad (34)$$

wherein

$${}^{n+1}\dot{\xi} \stackrel{\text{def}}{=} \left[ \mathbf{I} - \frac{1}{2}\Delta t {}^n\mathbf{Q} \right]^{-1} \cdot {}^n\mathbf{Q} \cdot \left[ \frac{1}{2}\Delta t {}^n\mathbf{Q} \cdot {}^n\xi + {}^n\xi \right] . \quad (35)$$

Using this approach facilitates to solve the presented system with high efficiency, while the numerical stability is significantly improved compared to other explicit integration schemes such as forward-Euler. After the updated volume fractions are computed, the intermediate plastic strains  ${}^n\tilde{\varepsilon}_{\text{pl}}^\alpha$  and  ${}^n\tilde{\varepsilon}_{\text{pl}}^\beta$  solely resulting from the phase-transformation can be obtained from (27) and (29) as described in Section 2.3.

Besides that, the time-integration of the differential equations governing the evolution of plastic strain in each phase is carried out using a backward-Euler time integration scheme (compare, e.g., Simo and Hughes (1998)). The discrete update of the plastic strains from timestep  ${}^n t$  to  ${}^{n+1}t$  according to (15) yields

$${}^{n+1}\varepsilon_{\text{pl}}^\alpha = {}^n\varepsilon_{\text{pl}}^\alpha + {}^{n+1}\lambda^\alpha \text{sgn} \left( {}^{n+1}q_{\text{pl},\psi}^\alpha - {}^{n+1}\xi^\alpha b^\alpha \right) , \quad (36)$$

with  ${}^{n+1}\varepsilon_{\text{pl}}^\alpha = \widehat{\varepsilon}_{\text{pl}}^\alpha(t = {}^{n+1}t)$  the updated plastic strains,  ${}^n\tilde{\varepsilon}_{\text{pl}}^\alpha$  the current intermediate plastic strain resulting from phase-transformation,  ${}^{n+1}\lambda^\alpha = \Delta t \dot{\lambda}^\alpha \in \mathbb{R}^+$  the current Langrangian multiplier, and  $\text{sgn}({}^{n+1}q_{\text{pl},\psi}^\alpha - {}^{n+1}\xi^\alpha b^\alpha)$  the sign of the plastic driving force—being reduced by the back stress  ${}^{n+1}\xi^\alpha b^\alpha$ —assigned to phase  $\alpha$  at time  $t = {}^{n+1}t$ .

In the current context, the Lagrangian multiplier can be expressed in terms of the trial value of the yield function  $\Phi_{\text{tri}}^\alpha = \widehat{\Phi}^\alpha(q_{\text{pl},\psi,\text{tri}}^\alpha, {}^n Y^\alpha)$ , with the trial plastic driving force  $q_{\text{pl},\psi,\text{tri}}^\alpha$  and  ${}^n Y^\alpha = \widehat{Y}^\alpha({}^n \gamma^\alpha)$  the yield stress of phase  $\alpha$  at time  $t = {}^n t$ . For the derivation of the trial plastic driving force, we make use of the intermediate state potential  $\widehat{\Psi} \stackrel{\text{def}}{=} \widehat{\Psi}({}^{n+1} \varepsilon, {}^n \varepsilon_{\text{pl}}^{\text{1d}}, \theta, {}^{n+1} \xi)$ , where the updated volume fractions  ${}^{n+1} \xi$  obtained from the phase-transformation algorithm, (34) and (35), are considered. Thus, the trial plastic driving force for phase  $\alpha$  results in

$$\begin{aligned} q_{\text{pl},\psi,\text{tri}}^\alpha &= - \left. \frac{\partial \widehat{\Psi}({}^{n+1} \varepsilon, {}^n \varepsilon_{\text{pl}}^{\text{1d}}, \theta, {}^{n+1} \xi)}{\partial {}^n \varepsilon_{\text{pl}}^\alpha} \right|_\theta \\ &= - \left. \frac{\partial}{\partial {}^n \varepsilon_{\text{pl}}^\alpha} \right|_\theta \sum_\alpha {}^{n+1} \xi^\alpha \widehat{\psi}^\alpha({}^{n+1} \varepsilon, {}^n \varepsilon_{\text{pl}}^\alpha, \theta) \\ &= - {}^{n+1} \xi^\alpha \left. \frac{\partial \widehat{\psi}^\alpha({}^{n+1} \varepsilon, {}^n \varepsilon_{\text{pl}}^\alpha, \theta)}{\partial {}^n \varepsilon_{\text{pl}}^\alpha} \right|_\theta . \end{aligned} \quad (37)$$

Based on this, the trial value  $\Phi_{\text{tri}}^\alpha$  of the yield function can be evaluated, facilitating to express the Lagrangian multiplier as

$${}^{n+1} \lambda^\alpha = \frac{\Phi_{\text{tri}}^\alpha}{{}^{n+1} \xi^\alpha [\mathbf{E}^\alpha + H^\alpha]} . \quad (38)$$

The plastic strains  $\varepsilon_{\text{pl}}^\alpha$  in each phase  $\alpha$  can then be updated from time  ${}^n t$  to  ${}^{n+1} t$  in an explicit manner according to (36), while the accumulated plastic strains  ${}^{n+1} \gamma^\alpha$  are obtained from

$${}^{n+1} \gamma^\alpha = {}^n \gamma^\alpha + {}^{n+1} \lambda^\alpha . \quad (39)$$

Here, the consistency of history variables is accounted for by considering the intermediate accumulated plastic strains

$${}^n \tilde{\gamma}^\alpha = \widehat{\gamma}^\alpha({}^n \gamma^\alpha, {}^n \varepsilon_{\text{pl}}^\alpha, {}^n \varepsilon_{\text{pl}}^\alpha) \stackrel{\text{def}}{=} {}^n \gamma^\alpha + |{}^n \varepsilon_{\text{pl}}^\alpha - {}^n \varepsilon_{\text{pl}}^\alpha| . \quad (40)$$

Moreover, note that the change of plastic strains due to inheritance can be expressed in terms of

$$\Delta \varepsilon_{\text{pl},\text{inh}}^\alpha \stackrel{\text{def}}{=} \varepsilon_{\text{pl}}^\alpha - \varepsilon_{\text{pl}}^\alpha . \quad (41)$$

A flowchart visualizing the actual algorithmical implementation is provided in Appendix A in terms of a Nassi-Shneiderman diagramme.

#### 4. Numerical Examples

This section provides several numerical examples for the model presented in Section 2, where we consider homogeneous deformation states at constant temperature using a quasi-static strain rate of  $\dot{\varepsilon} = 10^{-4} \text{ s}^{-1}$ . In Section 4.1 we show the behaviour of the phase-transformation model without consideration of plasticity, illustrating that the implemented phase transformation model works correctly.

Then, in Section 4.2 the interactions between phase-transformations and plasticity are evaluated. In particular, two numerical examples are addressed, highlighting the influence of concave and convex plastic inheritance functions. For these examples we restrict ourselves to the tensile regime in stress space, since we in this work only consider a martensitic tension phase for simplicity.

In Section 4.3 we investigate the behaviour of the phase-transformation-plasticity model when applied to material parameters corresponding to TRIP steel (see Table 2). Note that TRIP (transformation induced plasticity) steel particularly involves higher martensitic transformation strains. Here, we once more focus on the tensile regime, where the results are restricted to non-negative stresses as in the case of shape memory alloys.

##### 4.1. Shape memory alloys: phase-transformations without plasticity

Figure 4 displays the stress-strain response of SMA at different temperatures. In order to show that the model properly describes the temperature-dependent pseudo-elastic response of SMA, we compute the stress-strain response at  $\theta = 263 \text{ K}$ , Figure 4 (a), and  $\theta = 323 \text{ K}$ , Figure 4 (b), using parameters as suggested in Govindjee and Hall (2000) and a maximum strain of  $\varepsilon_{\text{max}} = 0.08$ .

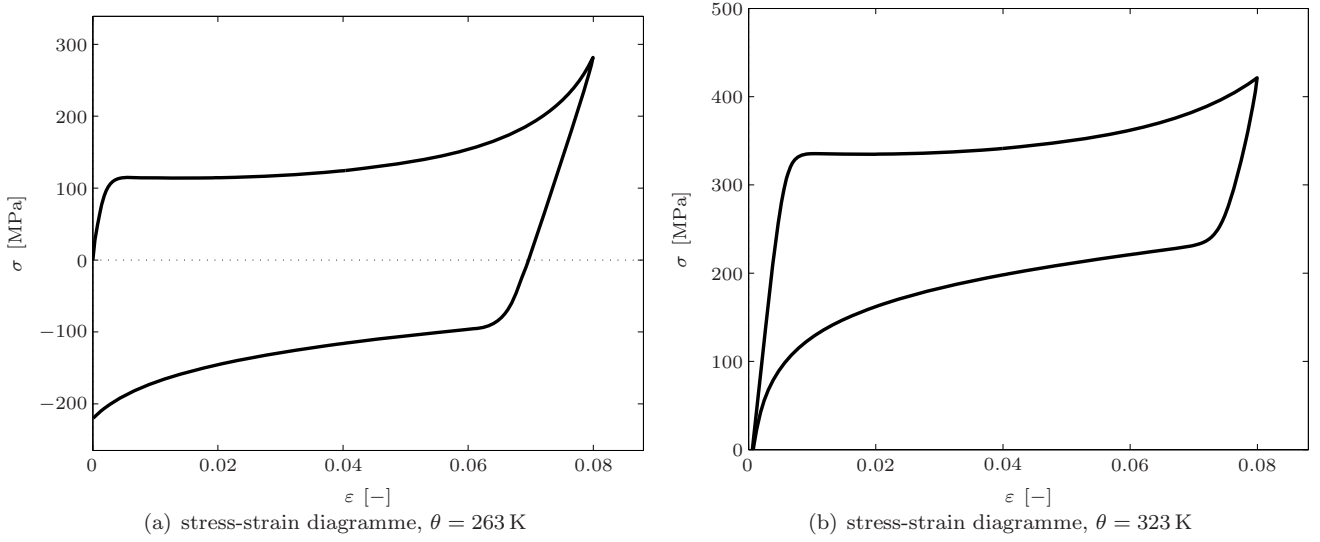


Figure 4: Phase-transformations without plasticity in SMA: pseudo-plastic response as observed at low temperatures,  $\theta = 263$  K (a) and pseudo-elastic response as observed at high temperatures,  $\theta = 323$  K (b), cf. Govindjee and Hall (2000).

#### 4.2. Shape memory alloys: phase-transformations with plasticity

In contrast to the non-plastic response provided in Section 4.1, we now make use of the material parameters provided in Table 1. In particular, we now investigate the behaviour of the model at a constant temperature of  $\theta = 283$  K. As initial conditions, we assume the material to consist of pure austenite, i.e.  ${}^0\xi = [\xi^A|_0, \xi^M|_0]^t = [1, 0]^t$ . The material is then loaded by applying a strain of  $\hat{\varepsilon}(t) = \hat{\tau}(t) \varepsilon_{\max}$ , where  $\hat{\tau}(t) \subset \mathbb{R}$  is a time-scaling function and  $\varepsilon_{\max} = 0.05$  is the maximum applied strain.

Figure 5 shows the results obtained for a concave inheritance probability function, where we restrict ourselves to the tensile regime, i.e.  $\sigma > 0$ . As a tensile load is applied, martensite starts to evolve (see Figure 5(b)), while both material phases initially behave elastically ( $\varepsilon_{\text{pl}}^A = \varepsilon_{\text{pl}}^M = 0$  as  $\varepsilon < 0.0175$ , compare Figure 5(c)). At  $\varepsilon \approx 0.0175$ , plastic flow in the austenitic phase is initiated, and at  $\varepsilon \approx 0.0225$  also martensite starts to deform plastically, such that  $\varepsilon_{\text{pl}}^A > \varepsilon_{\text{pl}}^M$  (Figure 5(c)). The simultaneous plastic flow of both material phases can also be seen in the stress-strain diagramme (Figure 5(a)) showing a linear proportional hardening behaviour for  $\varepsilon \in [0.0225, 0.05]$ .

As austenite possesses a higher plastic strain than martensite during the first tensile load cycle ( $\varepsilon_{\text{pl}}^A > \varepsilon_{\text{pl}}^M$  for  $\varepsilon \in [0.0225, 0.05]$ , compare Figure 5(c)), the evolving martensitic phase (Figure 5(b)) inherits additional plastic strains present in the austenitic phase. However, the change of plastic strains due to inheritance is very small as long as the change of plastic strains is mainly governed by the plastic evolution law (15), see Figure 5(d).

As the maximum strain of  $\varepsilon = 0.05$  is reached, the load reverses. At this point also the phase-transformations start to revert. As shown in Figure 5(b), the volume fraction of martensite starts to decrease, while the austenitic phase is now evolving. Furthermore, the evolution of plasticity stops—the change of plastic strains is now solely driven by inheritance resulting from the evolution of the austenitic phase, see Figure 5(b). Due to the concave inheritance function applied, a part of the plastic strains is pushed to the martensitic phase, while the other part is inherited by austenite. Physically speaking, the dislocations pushed by the phase front lead to an increased plastic distortion of the martensitic phase such that the martensitic plastic strains increase (compare Figure 5(c)). On the other hand, at  $\varepsilon = 0.05$  the martensitic plastic strains are smaller than those in austenite. Thus the inheritance initially leads to a decrease of plastic strains in austenite. As the martensitic plastic strains increase further, at  $\varepsilon \approx 0.03$  also the austenitic plastic strains start to increase again. Then, at  $\varepsilon \approx 0.0225$ , the stress reaches  $\sigma = 0$  (see Figure 5(a)) and the load cycle is completed.

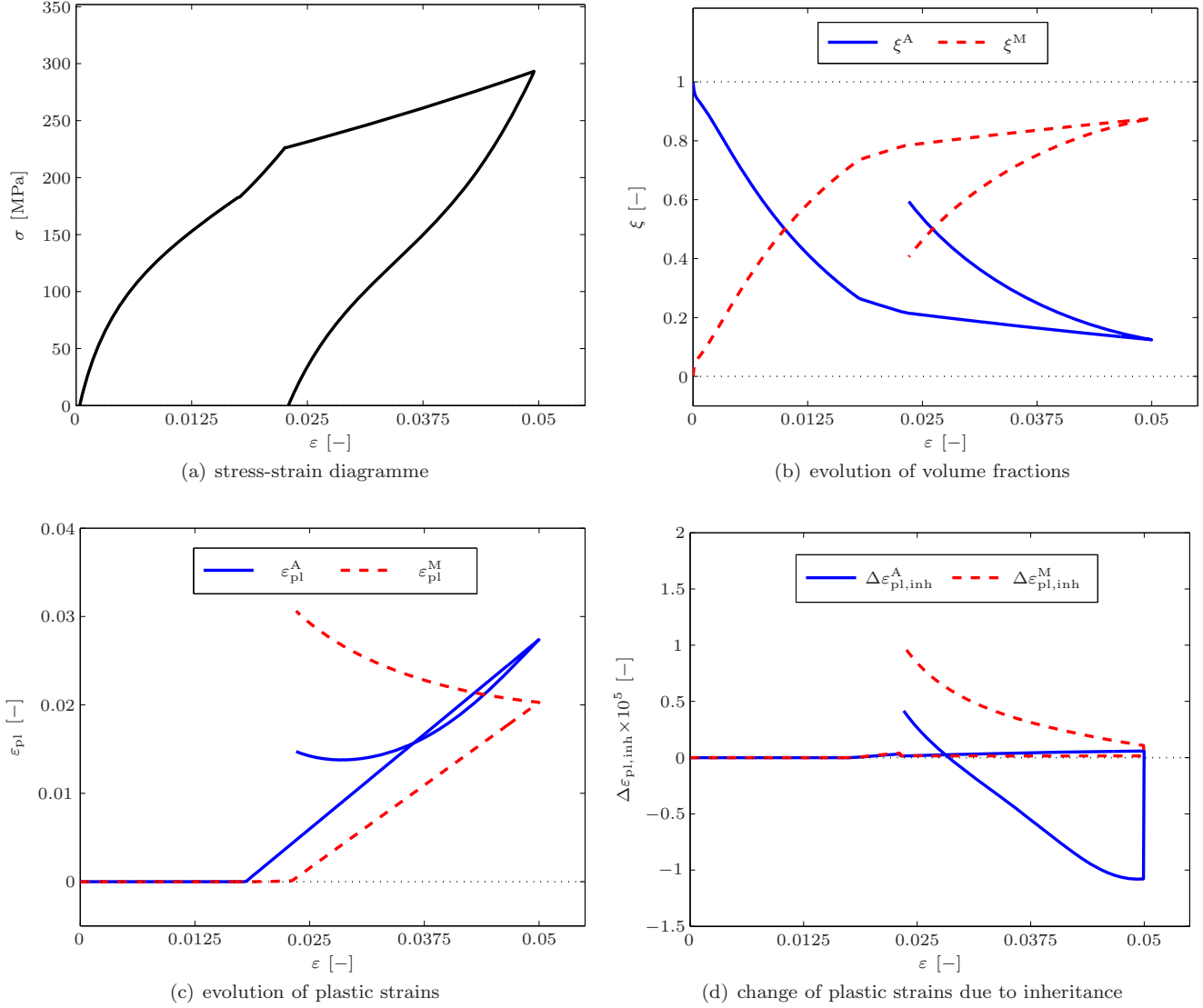


Figure 5: Phase-transformations in SMA: stress-strain diagramme (a), evolution of volume fractions (b), evolution of plastic strains (c) and change of plastic strains due to inheritance (d) resulting from the evolution of phases obtained by applying a maximum tension of  $\varepsilon_{\max} = 0.05$ . Note that concave inheritance probability functions  $\Pi^{A \rightarrow M} = \hat{\Pi}_{ccv}^{A \rightarrow M}(\xi^A, \varepsilon_{pl}^A; \kappa = 0.05, \varepsilon_{pl,sat}^A = 0.1)$  and  $\Pi^{M \rightarrow A} = \hat{\Pi}_{ccv}^{M \rightarrow A}(\xi^M, \varepsilon_{pl}^M; \kappa = 0.05, \varepsilon_{pl,sat}^M = 0.1)$  are chosen here (see Figure 3). The calculations are done at constant temperature of  $\theta = 283$  K.

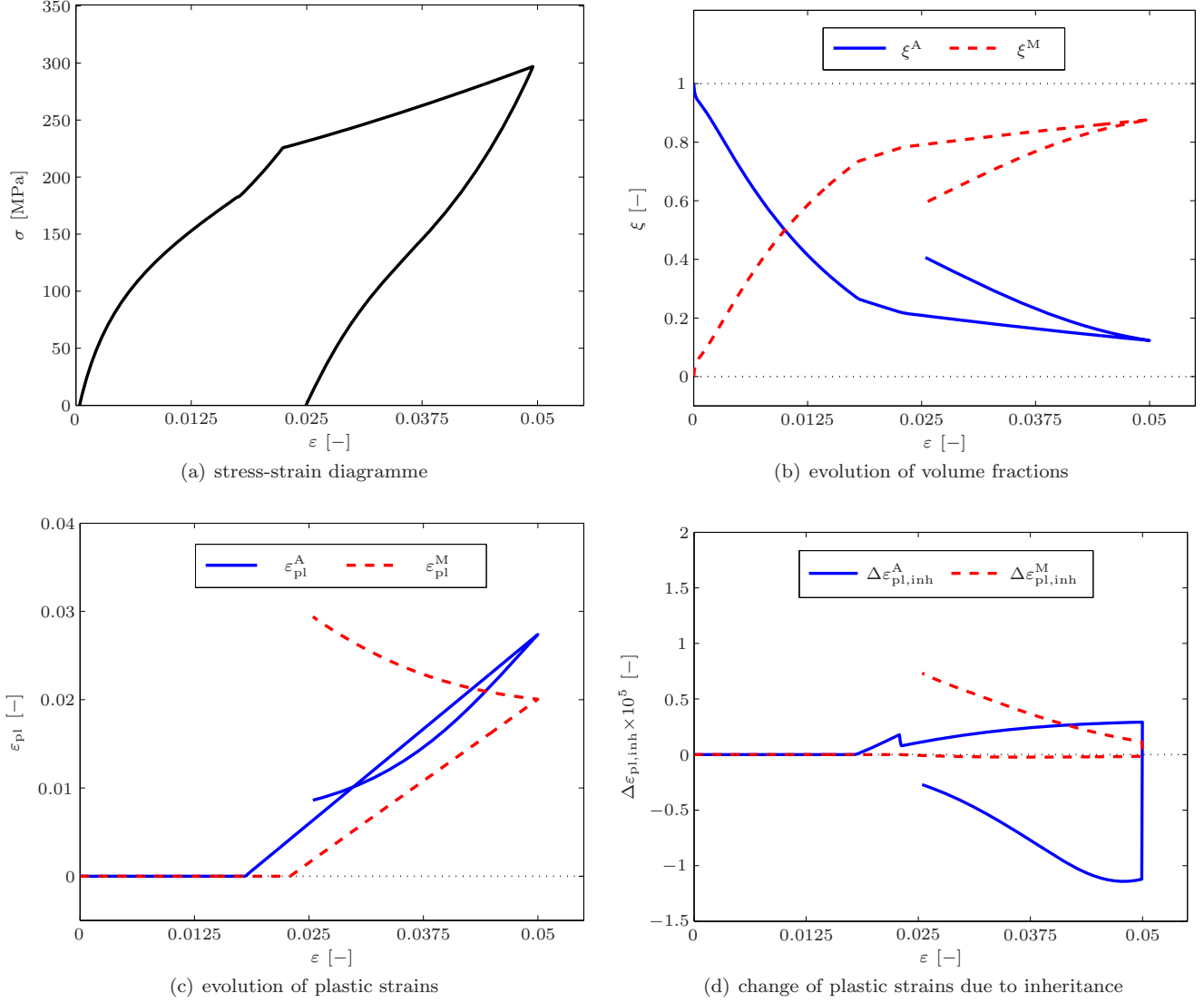


Figure 6: Phase-transformations in SMA: stress-strain diagramme (a), evolution of volume fractions (b), evolution of plastic strains (c) and change of plastic strains due to inheritance (d) resulting from the evolution of phases obtained by applying a maximum tension of  $\varepsilon_{\max} = 0.05$ . Note that convex inheritance probability functions  $\Pi^{A \rightarrow M} = \widehat{\Pi}_{cvx}^{A \rightarrow M}(\xi^A, \varepsilon_{pl}^A; \kappa = 0.1)$  and  $\Pi^{M \rightarrow A} = \widehat{\Pi}_{cvx}^{M \rightarrow A}(\xi^M, \varepsilon_{pl}^M; \kappa = 0.1)$  are chosen here (see Figure 2). The calculations are done at constant temperature of  $\theta = 283$  K.

Assuming a convex inheritance probability function means that dislocations are rather pushed than inherited by trend (compare Figures 2 and 3). Figure 6 provides the results obtained for SMA using a convex inheritance probability function. Comparison of Figures 6(c) and 5(c) shows that the convex inheritance function leads to a slightly stronger increase of plastic strains in martensite, with at the same time stronger decrease of plastic strains in austenite. This corresponds to the assumption, that—by trend—the convex inheritance function rather pushes dislocations to the decreasing phase, while less dislocations remain for inheritance by the increasing phase. Comparison of Figures 6(a) and 5(a) and Figures 6(b) and 5(b), respectively, shows that the plastic inheritance function has an influence also on the macroscopic response of the material. Not only the zero stress state is reached at different strains, but also the evolution of phases differs. To be specific, after reverting the load austenite is much more likely to evolve assuming concave inheritance, while for convex inheritance the austenitic volume fraction evolves with less intensity (compare Figures 5(b) and 6(b)).

#### 4.3. TRIP steel: phase-transformations with plasticity

Apart from SMA, we also investigate the behaviour of the material model when material constants as provided in Table 2 are applied. These are adapted to what is known for TRIP steels. As initial conditions, we once more assume the material to consist of pure austenite, i.e.  ${}^0\xi = [\xi^A|_0, \xi^M|_0]^t = [1, 0]^t$ . Furthermore, we restrict ourselves to the tensile regime and non-negative stresses in the following. The calculation is done at a constant temperature of  $\theta = 283\text{ K}$ .

Figure 7 shows the results obtained for a concave inheritance probability function. Initially, the material behaves purely elastic, as neither phase-transformations occur nor plastic strains evolve, see Figures 7(b) and (c), respectively. Then, at a strain of  $\varepsilon \approx 0.005$ , austenite starts to deform plastically, Figure 7(c). A further increase of the applied strain leads to an evolution of the martensitic tensile phase, Figure 7(b), while both phases and thus the overall macroscopic material is undergoing plastic flow as observed in experiments. As the load reverses, the volume fractions as well as the plastic strains remain constant, resulting in a purely elastic deformation back to the unloaded state at which external forces vanish identically, i.e.  $\sigma = 0$ . This result coincides with the experimentally-observed fact that TRIP steels do not show the pseudo-elastic hysteresis behaviour as in the case of SMA. Comparison of Figures 5(b) and 5(c) and 7(b) and 7(c), respectively, shows that for shape memory alloys the material transforms first and then yields, while when applied to TRIP steel the model predicts that the material yields first and then starts to transform.

## 5. Summary

The main goal of this work is to develop a coupled model for the interaction of phase-transformations and plasticity. As a basis, we make use of a one-dimensional micromechanically motivated potential-based phase-transformation model. Based on this model, we extend the Helmholtz free energy function of the material in order to account for the influence of evolving plastic strains. Furthermore, we use a von-Mises type plasticity model in terms of the driving forces for each phase as related to the overall potential. For the plasticity model, we consider linear proportional hardening, facilitating to transpose the backward-Euler based evolution law in such way, that explicit updates of the plastic strains as well as plastic history variables are enabled in each load step. Together with the A-stable explicit update of the volume fractions, the overall model turns out to be numerically efficient.

The influence of the inheritance probability function is discussed in detail for SMA, where it is shown, that the type of inheritance law has an influence not only on the macroscopic stress response, but also on the evolution of volume fractions. Besides the application to SMA, we also apply the model to TRIP steel material parameters. In case of TRIP steel, the correlation between simulated stress-strain response and experimentally observed stress-strain behaviour shows a good agreement, where in particular the ongoing hardening up to large strains is represented by the model, see e.g. Choi *et al.* (2009). It turns out that for SMA the material first transforms and then yields, while for TRIP the material first yields and then starts to transform. Although the underlying phase-transformation model was originally established for SMA, see Govindjee and Hall (2000), the application of the coupled phase-transformation plasticity model to TRIP steel gives promising results in view of future enhancements of the model.

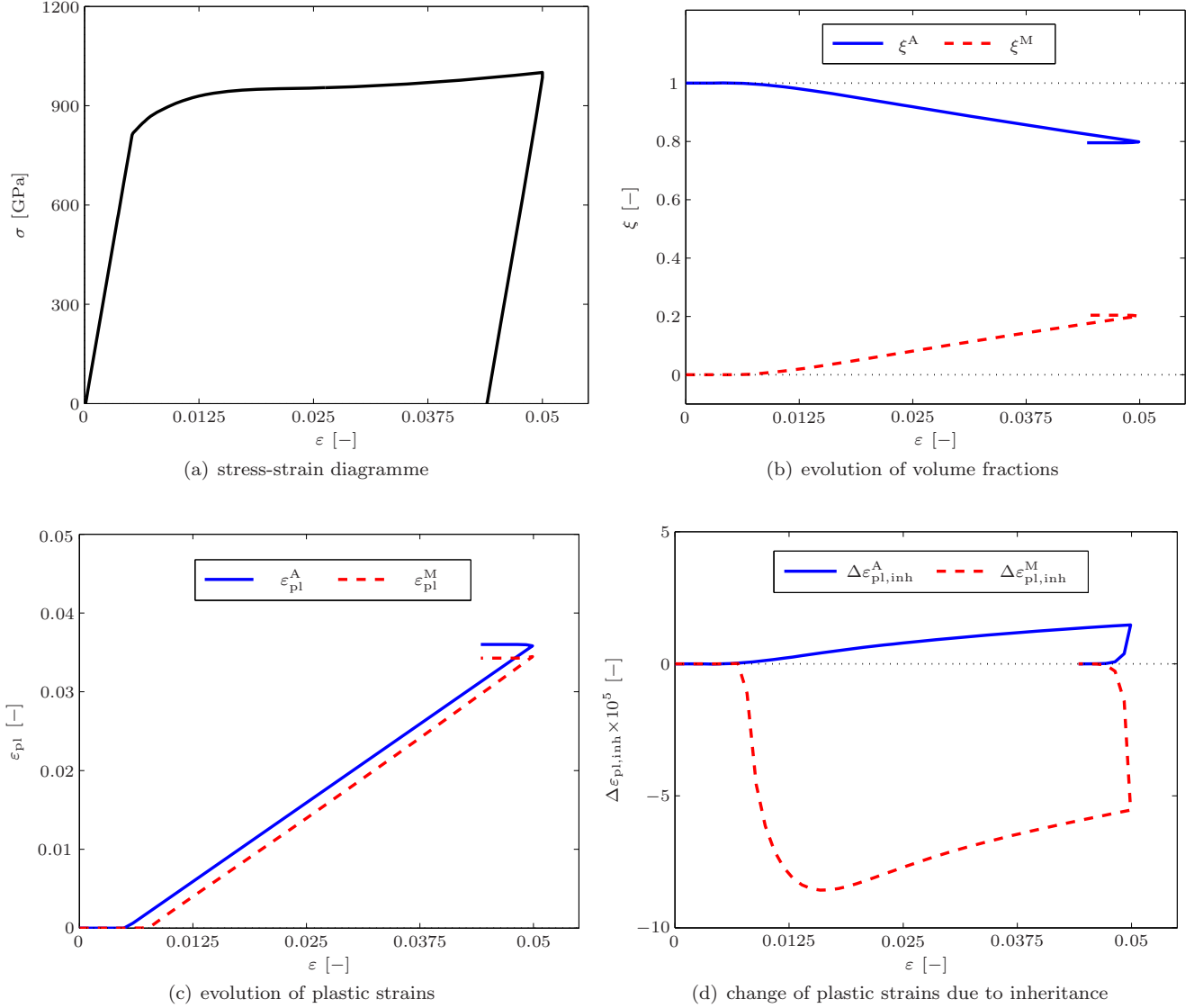


Figure 7: Model based on TRIP steel material parameters: stress-strain diagramme (a), evolution of volume fractions (b), evolution of plastic strains (c) and change of plastic strains due to inheritance (d) resulting from the evolution of phases obtained by applying a maximum tension of  $\varepsilon_{\max} = 0.05$ . Note that concave inheritance probability functions  $\Pi^{A \rightarrow M} = \widehat{\Pi}_{\text{ccv}}^{A \rightarrow M}(\xi^M, \varepsilon_{\text{pl}}^M; \kappa = 0.05, \varepsilon_{\text{pl,sat}}^M = 0.1)$  and  $\Pi^{M \rightarrow A} = \widehat{\Pi}_{\text{ccv}}^{M \rightarrow A}(\xi^A, \varepsilon_{\text{pl}}^A; \kappa = 0.05, \varepsilon_{\text{pl,sat}}^A = 0.1)$  are chosen here (see Figure 3). The calculations are done at constant temperature of  $\theta = 283 \text{ K}$ .

For future work, the correlation between simulation and experiment is expected to become more exact by additionally taking into account thermo-mechanical coupling effects occurring during phase-transformations. Furthermore, the consideration of a martensitic compression phase, as discussed in Ostwald *et al.* (2010), is also expected to increase the accuracy of the simulation results and facilitates to take into account the compression regime in addition. Also an extension of the model to the three-dimensional case, e.g. by means of a micro-sphere approach, will contribute to a smoothening of the macroscopic material response.

As elaborated in Section 4, the chosen inheritance law has a severe influence on the macroscopic material response. To this end, it is necessary to carry out detailed micro-mechanical experiments that reveal the complex interactions between evolving phase fronts and moving dislocations, eventually giving insight to the physical inheritance probability law depending on the volume fractions and dislocation densities as well as—in general—also on the temperatures of the involved phases.

### **Acknowledgements**

The support of the Deutsche Forschungsgemeinschaft (DFG), that made possible to develop this research within the research project TRR30 B6, is gratefully acknowledged.

*please turn overleaf...*

## A Algorithmic flowchart

## Numerical scheme — coupling of phase-transformations and plasticity

while $t < t_{\max}$ do	
set $t = {}^{n+1}t = {}^n t + \Delta t \in [0, t_{\max}]$	
given: ${}^n \boldsymbol{\xi} = [{}^n \xi^A, {}^n \xi^M]^t$ , ${}^n \boldsymbol{\varepsilon}_{\text{pl}}^{1d} = [{}^n \varepsilon_{\text{pl}}^A, {}^n \varepsilon_{\text{pl}}^M]^t$ , ${}^n \boldsymbol{\gamma} = [{}^n \gamma^A, {}^n \gamma^M]^t$ , ${}^{n+1} \boldsymbol{\varepsilon}$	
obtain ${}^{n+1} \boldsymbol{\xi}$ from (34) and (35).	
check whether $\Delta \xi^M = {}^{n+1} \xi^M - {}^n \xi^M > 0$	
true	false
define increasing phase $\alpha \stackrel{\text{def}}{=} M$ and decreasing phase $\beta \stackrel{\text{def}}{=} A$	define increasing phase $\alpha \stackrel{\text{def}}{=} A$ and decreasing phase $\beta \stackrel{\text{def}}{=} M$
compute plastic inheritance probability $\Pi^{\beta \rightarrow \alpha} = \widehat{\Pi}^{\beta \rightarrow \alpha}({}^{n+1} \xi^\beta, {}^n \varepsilon_{\text{pl}}^\beta; \dots)$	
compute intermediate plastic strains ${}^n \tilde{\varepsilon}_{\text{pl}}^\alpha = \widehat{\varepsilon}_{\text{pl}}^\alpha({}^n \xi^\alpha, \Delta \xi^\alpha, {}^n \varepsilon_{\text{pl}}^\alpha, {}^n \varepsilon_{\text{pl}}^\beta, \Pi^{\beta \rightarrow \alpha})$ and ${}^n \tilde{\varepsilon}_{\text{pl}}^\beta = \widehat{\varepsilon}_{\text{pl}}^\beta({}^n \xi^\beta, \Delta \xi^\beta, {}^n \varepsilon_{\text{pl}}^\beta, \Pi^{\beta \rightarrow \alpha})$ solely resulting from the change of volume fractions according to (27) and (29)	
compute changes of plastic strains— $\Delta \varepsilon_{\text{pl,inh}}^\alpha$ and $\Delta \varepsilon_{\text{pl,inh}}^\beta$ —according to (41)	
compute consistent intermediate history variables ${}^n \tilde{\gamma}^\alpha = \widehat{\gamma}^\alpha({}^n \gamma^\alpha, {}^n \tilde{\varepsilon}_{\text{pl}}^\alpha, {}^n \varepsilon_{\text{pl}}^\alpha)$ and ${}^n \tilde{\gamma}^\beta = \widehat{\gamma}^\beta({}^n \gamma^\beta, {}^n \tilde{\varepsilon}_{\text{pl}}^\beta, {}^n \varepsilon_{\text{pl}}^\beta)$ according to (40)	
evaluate intermediate state potential $\tilde{\Psi} \stackrel{\text{def}}{=} \widehat{\Psi}({}^{n+1} \boldsymbol{\varepsilon}, {}^n \boldsymbol{\varepsilon}_{\text{pl}}^{1d}, \theta, {}^{n+1} \boldsymbol{\xi})$	
compute trial plastic driving forces $q_{\text{pl},\Psi,\text{tri}}^\alpha$ and $q_{\text{pl},\Psi,\text{tri}}^\beta$ and Lagrangian multipliers ${}^{n+1} \lambda^\alpha$ and ${}^{n+1} \lambda^\beta$ according to (37) and (38), respectively	
compute final updates for plastic strains and accumulated plastic strains according to (36) and (39)	
compute stress response ${}^{n+1} \boldsymbol{\sigma} = \left. \frac{\partial \widehat{\Psi}({}^{n+1} \boldsymbol{\varepsilon}, {}^{n+1} \boldsymbol{\varepsilon}_{\text{pl}}^{1d}, \theta, {}^{n+1} \boldsymbol{\xi})}{\partial {}^{n+1} \boldsymbol{\varepsilon}} \right _{\theta, {}^{n+1} \boldsymbol{\varepsilon}_{\text{pl}}^{1d}}$	
return ${}^{n+1} \boldsymbol{\xi}$ , ${}^{n+1} \boldsymbol{\varepsilon}_{\text{pl}}^{1d}$ , ${}^{n+1} \boldsymbol{\gamma}$ , ${}^{n+1} \boldsymbol{\sigma}$ and set $n \leftarrow n + 1$	

## B Material parameters

Table 1: SMA material parameters considered in Section 4.2 (compare, e.g., Govindjee and Hall (2000); Bhat-tacharya (2003)).

	material parameter	symbol	value
austenite A (parent phase):	Young's modulus	$E^A$	67 GPa
	hardening modulus	$H^A$	$E^A/6$
	initial yield stress	$Y_0^A$	1200 MPa
	transformation strain	$\varepsilon_{tr}^A$	0
	latent heat	$\lambda_T^A$	0
martensite M:	Young's modulus	$E^M$	26.3 GPa
	hardening modulus	$H^M$	$E^M/3$
	initial yield stress	$Y_0^M$	600 MPa
	transformation strain	$\varepsilon_{tr}^M$	0.025
	latent heat	$\lambda_T^M$	14500 J/kg
common parameters:	coefficient of thermal expansion	$\zeta$	$12 \times 10^{-7} \text{ K}^{-1}$
	reference temperature	$\theta_0$	273 K
	heat capacity	$c_p$	400 J/kgK
	transition attempt frequency	$\omega$	$1.6 \text{ s}^{-1}$
	transformation region's volume	$\Delta v$	$2.71 \times 10^{-18} \text{ mm}^3$
	Boltzmann's constant	$k$	$1.381 \times 10^{-23} \text{ J/K}$

Table 2: Specific TRIP steel material parameters considered (compare Lambers *et al.* (2009)).

	material parameter	symbol	value
austenite A (parent phase):	Young's modulus	$E^A$	160 GPa
	hardening modulus	$H^A$	$E^A/4$
	initial yield stress	$Y_0^A$	800 MPa
	transformation strain	$\varepsilon_{tr}^A$	0
martensite M:	Young's modulus	$E^M$	160 GPa
	hardening modulus	$H^M$	$E^M/12$
	initial yield stress	$Y_0^M$	1200 MPa
	transformation strain	$\varepsilon_{tr}^M$	0.04
common parameters:	transition attempt frequency	$\omega$	$16 \text{ s}^{-1}$

## References

- Abeyaratne, R., Kim, S. and Knowles, J. (1994). A one-dimensional continuum model for shape-memory alloys, *Int. J. Sol. Struct.* **31**, pp. 2229–2249.
- Abeyaratne, R. and Knowles, J. (1990). On the driving traction acting on a surface of strain discontinuity in a continuum, *J. Mech. Phys. Sol.* **38**, pp. 345–360.
- Abeyaratne, R. and Knowles, J. (1993). A continuum model of a thermoelastic solid capable of undergoing phase transitions, *J. Mech. Phys. Sol.* **41**, pp. 541–571.
- Abeyaratne, R. and Knowles, J. (1997). On the kinetics of an austenite  $\rightarrow$  martensite phase transformation induced by impact in a Cu-Al-Ni shape-memory alloy, *Acta Mater.* **45**, pp. 1671–1683.
- Achenbach, M. (1989). A model for an alloy with shape memory, *Int. J. Plast.* **5**, pp. 371–395.
- Auricchio, F. and Taylor, R. (1997). Shape-memory alloys: modelling and numerical simulations of the finite-strain superelastic behavior, *Comp. Meth. Appl. Mech. Engrg.* **143**, pp. 175–194.
- Bain, E. C. (1924). The nature of martensite, *Trans. AIME* **70**, p. 25.
- Ball, J. (1977). Convexity conditions and existence theorems in nonlinear elasticity, *Arch. Rat. Mech. Anal.* **63**, pp. 337–403.
- Bartel, T. and Hackl, K. (2009). A micromechanical model for martensitic phase-transformations in shape-memory alloys based on energy-relaxation, *Z. Angew. Math. Mech.* **89** (10), pp. 792–809, DOI: 10.1002/zamm.200900244.
- Berezovski, A. and Maugin, G. (2007). Moving singularities in thermoelastic solids, *Int. J. Fract.* **147**, pp. 191–198.
- Bhattacharya, K. (2003). *Microstructure of Martensite - Why it forms and how it gives rise to the shape-memory effect* (Oxford University Press, New York).
- Bowles, J. and MacKenzie, J. (1954). The crystallography of martensite transformations I and II, *Acta Metall.* **2**, pp. 129–137.
- Cherkaoui, M., Sun, Q. and Song, G. (2000). Micromechanics modeling of composite with ductile matrix and shape memory alloy reinforcement, *Int. J. Sol. Struct.* **37**, pp. 1577–1594.
- Choi, K., Liu, W., Sun, X. and Khaleel, M. (2009). Microstructure-based constitutive modeling of TRIP steel: Prediction of ductility and failure modes under different loading conditions, *Acta Mater.* **57**, pp. 2592–2604, DOI: 10.1016/j.actamat.2009.02.020.
- Dacorogna, B. (1989). *Direct Methods in the Calculus of Variations* (Springer, Berlin).
- DeSimone, A. and Dolzmann, G. (1999). Material instabilities in nematic polymers, *Physica D* **136**, pp. 175–191.
- Govindjee, S. and Hall, G. (2000). A computational model for shape memory alloys, *Int. J. Sol. Struct.* **37**, pp. 735–760.
- Helm, D. and Haupt, P. (2003). Shape memory behaviour: modelling within continuum mechanics, *Int. J. Sol. Struct.* **40**, pp. 827–849.
- Huo, Y. and Müller, I. (1993). Nonequilibrium thermodynamics of pseudoelasticity, *Cont. Mech. Thermodyn.* **5**, pp. 163–204.
- James, R. and Hane, K. (2000). Martensitic transformations and shape memory materials, *Acta Mater.* **48**, pp. 197–222.
- Kohn, R. (1991). The relaxation of a double-well energy, *Cont. Mech. Thermodyn.* **3**, pp. 193–236.
- Lambers, H.-G., Tschumak, S., Maier, H.-J. and Canadinc, D. (2009). Tensile properties of 51crv4 steel in martensitic, bainitic and austenitic state, *Hot Sheet Metal Forming of High-Performance Steel* **2**, pp. 73–82.
- Maugin, G. and Berezovski, A. (2009). On the propagation of singular surfaces in thermoelasticity, *J. Therm. Stresses* **32**, pp. 557–592.
- Miehe, C., Lambrecht, M. and Gürses, E. (2004). Analysis of material instabilities in inelastic solids by incremental energy minimization and relaxation methods: evolving deformation microstructures in finite plasticity, *J. Mech. Phys. Sol.* **52**, pp. 2725–2769, DOI: 10.1016/j.jmps.2004.05.011.
- Mielke, A. and Theil, F. (1999). A mathematical model for rate-independent phase transformations with hysteresis, in H.-D. Alber, R. Balean and R. Farwig (eds.), *Proceedings of the Workshop on Models of Continuum Mechanics in Analysis and Engineering*.

- Mielke, A., Theil, F. and Levitas, V. (2002). A variational formulation of rate-independent phase transformations using an extremum principle, *Arch. Rat. Mech. Anal.* **162** (2), pp. 137–177.
- Morrey, C. (1952). Quasi-convexity and the lower semicontinuity of multiple integrals, *Pacific J. Math.* **2**, pp. 25–53.
- Müller, C. and Bruhns, O. (2006). A thermodynamic finite-strain model for pseudoelastic shape memory alloys, *Int. J. Plast.* **22**, pp. 1658–1682.
- Müller, I. and Seelecke, S. (2001). Thermodynamic aspects of shape memory alloys, *Math. Comp. Model.* **34**, pp. 1307–1355.
- Ortiz, M. and Repetto, E. (1999). Nonconvex energy minimization and dislocation structures in ductile single crystals, *J. Mech. Phys. Sol.* **47**, pp. 397–462.
- Ostwald, R., Bartel, T. and Menzel, A. (2010). A computational micro-sphere model applied to the simulation of phase-transformations, *J. Appl. Math. Mech.* **90**, pp. 605–622, DOI: 10.1002/zamm.200900390.
- Pagano, S., Alart, P. and Maisonneuve, O. (1998). Solid-solid phase transition modelling. local and global minimizations of non-convex and relaxed potentials. isothermal case for shape memory alloys, *Int. J. Eng. Sci.* **36**, pp. 1143–1172.
- Raniecki, B., LExcellent, C. and Tanaka, K. (1992). Thermodynamic models of pseudoelastic behaviour of shape memory alloys, *Arch. Mech.* **44**, pp. 261–284.
- Seelecke, S. (1996). Equilibrium thermodynamics of pseudoelasticity and quasiplasticity, *Cont. Mech. Thermodyn.* **8**, pp. 309–322.
- Simo, J. C. and Hughes, T. J. R. (1998). *Computational Inelasticity*, Interdisciplinary Applied Mathematics (Springer).
- Stupkiewicz, S. and Petryk, H. (2002). Modelling of laminated microstructures in stress-induced martensitic transformations, *J. Mech. Phys. Sol.* **50**, pp. 2303–2331.
- Sun, Q. and Hwang, K. (1993). Micromechanics modelling for the constitutive behavior of polycrystalline shape memory alloys-i. derivation of general relations, *J. Mech. Phys. Sol.* **41**, pp. 1–17.
- Sun, Q., Hwang, K. and Yu, S. (1991). A micromechanics constitutive model of transformation plasticity with shear and dilatation effect, *J. Mech. Phys. Sol.* **39**, pp. 507–524.
- Truesdell, C. and Toupin, R. (1960). The classical field theories, in *Handbuch der Physik* (Springer, Berlin).